

Received:
14 January 2020

Revised:
16 June 2020

Accepted:
24 June 2020

<https://doi.org/10.1259/bjr.20200064>

Cite this article as:

Paño B, Soler A, Goldman DA, Salvador R, Buñesch L, Sebastià C, et al. Usefulness of multidetector computed tomography to differentiate between renal cell carcinoma and oncocytoma. A model validation. *Br J Radiol* 2020; **93**: 20200064.

FULL PAPER

Usefulness of multidetector computed tomography to differentiate between renal cell carcinoma and oncocytoma. A model validation

¹BLANCA PAÑO, MD, ¹ALEXANDRE SOLER, MD, ²DEBRA A GOLDMAN, MD, ¹RAFAEL SALVADOR, MD, ¹LAURA BUÑESCH, MD, ¹CARMEN SEBASTIÀ, MD and CARLOS NICOLAU, MD

¹Department of Radiology, Hospital Clínic de Barcelona. 170, Villarroel street, 08036, Barcelona, Spain

²Department of Epidemiology & Biostatistics, Memorial Sloan Kettering Cancer Center, NY, USA

Address correspondence to: Dr Blanca Paño
E-mail: bpano@clinic.cat

Objective: The purpose of this study is to validate a multivariable predictive model previously developed to differentiate between renal cell carcinoma (RCC) and oncocytoma using CT parameters.

Methods and materials: We included 100 renal lesions with final diagnosis of RCC or oncocytoma studied before surgery with 4-phase multidetector CT (MDCT). We evaluated the characteristics of the tumors and the enhancement patterns at baseline, arterial, nephrographic and excretory MDCT phases.

Results: Histopathologically 15 tumors were oncocytomas and 85 RCCs. RCCs were significantly larger (median 4.4 cm vs 2.8 cm, $p = 0.006$). There were significant differences in nodule attenuation in the excretory phase compared to baseline (median: 31 vs 42, $p = 0.015$), with RCCs having lower values. Heterogeneous enhancement patterns were also more frequent in RCCs (85.9% vs 60%, $p = 0.027$).

Multivariable analysis showed that the independent predictors of malignancy were the enhancement pattern, with oncocytomas being more homogeneous in the nephrographic phase [Odds Ratio (OR) 0.16 (95%

CI 0.03 to 0.75, $p = 0.02$)], nodule enhancement in the excretory phase compared to baseline, with RCCs showing lower enhancement [OR 0.96 (95% CI 0.93 to 0.99, $p = 0.005$)], and a size > 4 cm, with RCCs being larger [OR 5.89 (95% CI 1.10 to 31.58), $p = 0.038$].

Conclusion: The multivariable predictive model previously developed which combines different MDCT parameters, including lesion size > 4 cm, lesion enhancement in the excretory phase compared to baseline and enhancement heterogeneity, can be successfully applied to distinguish RCC from oncocytoma.

Advances in knowledge: This study confirms that multiparametric assessment using MDCT (including parameters such as size, homogeneity and enhancement differences between the excretory and the baseline phases) can help distinguish between RCCs and oncocytomas. While it is true that this multiparametric predictive model may not always correctly classify renal tumors such as RCC or oncocytoma, it can be used to determine which patients would benefit from pre-surgical biopsy to confirm that the tumor is in fact an oncocytoma, and thereby avoid unnecessary surgical treatments.

INTRODUCTION

Renal cancer is among the 10 most common cancers in both males and females. For reasons that are not totally clear, the rate of new kidney cancers has been rising since the 1990 s, although this seems to have leveled off in the last few years. Part of this rise is probably due to the use of newer imaging tests such as CT scans, which are able to identify some cancers which may have otherwise remained undetected.¹

The accuracy of current imaging techniques in differentiating between renal cell carcinoma (RCC) and some

benign tumors such as oncocytoma, which account for 3–5% of all renal neoplasms in adults^{2–4} is low. In fact, differentiation between RCC and oncocytomas is usually based on the histologic findings of the surgically removed tumor. This difficulty in differentiating between RCC and oncocytomas using imaging techniques is due to the increased vascularity of these lesions, showing enhancement and washout, with reduced enhancement in the nephrographic phase leading to RCCs being mistakenly identified as oncocytomas in multidetector CT (MDCT) studies. In a previous study, a multivariable predictive model was developed to better differentiate these tumors

⁵ by combining different imaging parameters instead of addressing each parameter separately as previously reported in the literature. However, this model required validation in further studies. The purpose of this study is to validate a multi-variable predictive model previously developed to differentiate between RCC and oncocytoma using CT parameters.

METHODS AND MATERIALS

Patients

In this retrospective study, we used our institutional database to identify consecutive patients who had undergone surgical management of renal tumors from August 2010 to December 2014. For the purposes of this study, no institutional review board approval was required.

Patients who had pre-operative CT evaluation as per renal mass protocol of our institution (Hospital Clinic de Barcelona) including four phases (unenhanced, corticomedullary, nephrographic and excretory) and had confirmed pathological diagnosis of either oncocytoma or RCC were included in this retrospective study.

A total of 99 patients and 100 lesions were included. One patient had two lesions (two oncocytomas). Seven patients were excluded because the scans were performed with a different protocol.

CT examination

The majority of MDCT studies were performed using a 64-row helical scanner (37 patients), a 2-row helical scanner (19 patients) (Somatom Sensation 64 and Emotion Duo, respectively, both from Siemens Medical Solutions, Erlangen, Germany) and a Dual Source 128-row scanner (31 patients) (Somatom Definition Flash, Siemens Medical Solutions, Erlangen, Germany). The scan parameters of the MDCT studies performed in our department are shown in Table 1. 13 of the 99 CT scans were not performed in our institution, although those 13 patients had the same scan protocol of our center for renal mass characterization//but following a similar protocol (same phases, slice thickness and other technical parameters). All images were obtained in a single breath-hold using automatic tube current modulation (Care Dose 4D, Siemens Healthcare). Slices with a thickness of 5 mm and 2 mm were reconstructed in the axial plane in all phases. 20 min before the study, all patients drank 500 ml of diluted oral

contrast (Gastrografin, Bayer, 2%). All the studies involved the following phases: unenhanced, corticomedullary, nephrographic and excretory. Patients underwent unenhanced scanning of the abdomen down to the iliac crest. Patients also received 100 ml of non-ionic iohexol (Iopromide 300 mg I/mL; Bayer) injected with a power injector at a rate of 3 ml s⁻¹ using a bolus tracking algorithm (CareBolus, Siemens Medical Solutions; SmartPrep, GE Medical Systems) to calculate the bolus arrival time at the aorta. For bolus tracking, a threshold was set at 100 HU with a region of interest (ROI) located at the ascending aorta in the thoracoabdominal CT scans, and in the descending in the abdominal CT scans. Corticomedullary phase imaging was done 6 s after the threshold was reached. Nephrographic phase imaging was performed after 90 s after the start of injection. Excretory phase imaging was done after 3 min after the start of injection.

CT image analysis

Images were transferred to our picture archiving and communication system (RAIMSERVER) and were reviewed and analyzed using RAIM ALMA 3D software (2019; v. 4.2.2.6).

Two radiologists with 3 (AS, resident) and 9 (BP, genitourinary radiologist) years of experience in body radiology independently interpreted the CT studies and consensus was obtained in case of discrepancy. Both readers were aware of the presence of a renal tumor but were blinded to clinical and pathologic information.

The readers were asked to evaluate all the parameters included in the multivariable predictive model, on axial CT scan images (5 mm slices).

• Qualitative parameters

- Type of enhancement: homogeneous or heterogeneous (assessed in the nephrographic phase). Tumors with non-enhancing areas or with low attenuation areas were described as heterogeneous and tumors with uniform enhancement were described as homogeneous.

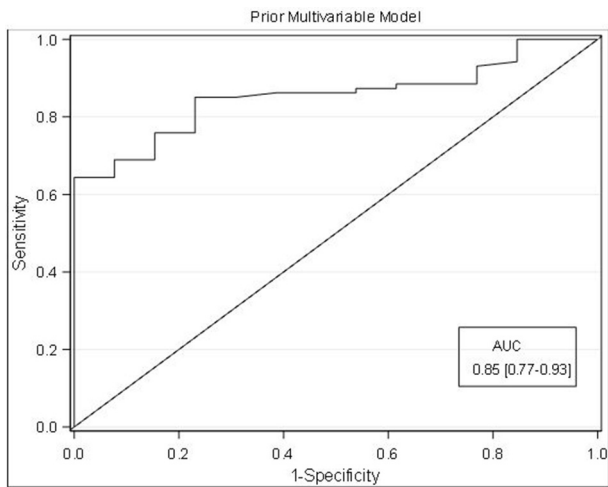
• Quantitative parameters

- Size: maximum diameter of the lesion in axial images.
- Attenuation value: the difference between the mean attenuation value for each nodule and the mean attenuation

Table 1. Scan parameters

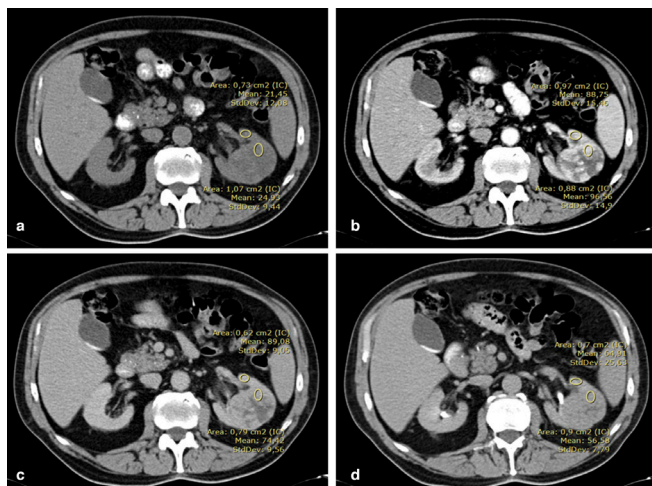
Parameters	128-row scanner	64-row scanner	2-row scanner
Detector colimation	128 × 1.2 mm	64 × 0.6 mm	2 × 4 mm
Effective section thickness	1.2 mm	0.6 mm	2 mm
Reconstruction increment	5 mm	5 mm	5 mm
Gantry rotation time	0.5 s	0.5 s	0.8 s
Pitch	0.6	1.35	1.6
Effective current	240 mAs	120 mAs	130 mAs
Tube voltage	120kVp	120 kVp	110 kVp
Kernel reconstruction	B20	B20	B40s

Figure 1. ROC curve for the prior multivariate model. AUC, area under the curve; ROC, receiver operating characteristic.



value in the baseline images was calculated for the excretory phase. For the analysis of the magnitude of enhancement, ROIs with a size between 0.5 and 1 cm² were placed on the most avid areas of enhancement of heterogeneous lesions, avoiding the focal hypoattenuating areas, and in the central area of homogeneous lesions (Figures 1 and 2). Enhancement differences during the excretory phase in relation to the unenhanced phase for absolute enhancement of the nodule were abbreviated as N3-N0.

Figure 2. Multiphasic MDCT study (A) unenhanced phase, (B) corticomedullary phase, (C) nephrographic phase and (D): excretory phase) of 79-year-old male shows a 5.3 cm solid lesion with heterogeneous contrast enhancement in the middle third of the left kidney. ROIs were placed on the lesion and on the renal cortex in each phase, calculating the mean attenuation \pm SD. This lesion corresponded to a clear cell subtype of RCC. MDCT, multidetector CT; RCC, renal cell carcinoma; ROI, region of interest; SD, standard deviation.



Prior multivariable model

For each lesion, we calculated the model equation constructed in the previous study. For values of X, the c regression coefficients are multiplied by 0 (no) or 1 (yes) for binary variables and by the actual continuous values otherwise:

$$\text{SCORE} = 5.3852 + (-1.7122 \times X_1) + (1.3891 \times X_2) + (-0.0758 \times X_3)$$

$$5.3852 = \text{slope}; -1.7122 = B_1; 1.3891 = B_2; -0.0758 = B_3$$

X_1 : Homogeneous enhancement (one if YES and 0 if NO).

X_2 : Size larger than 4 cm (one if YES and 0 if NO).

X_3 : Difference in attenuation for the excretory phase compared to the unenhanced phase (absolute value).

The predicted probability was derived from the standard logistic regression equation:

$$\text{prob} = \frac{1}{1 + e^{-\text{score}}}$$

As per mathematical nomenclature, e represents the exponent. The model provides the probability of a patient having RCC on a 0 to 1 scale, where 1 means having RCC and 0 means having oncocytoma. Therefore, for values closer to 1, the higher the probability of having RCC. An example of application is shown in Figure 3 .

Statistical analysis

Patient and imaging characteristics were described overall and by pathological type. One patient had two lesions and no adjustments were made for intra patient correlation.

All the descriptive data are expressed as median (range) and frequencies (%) unless specified otherwise. We validated the previously published model with receiver operative curve (ROC) analysis. We used the Wilcoxon Rank Sum test, Fisher's Exact test, and logistic regression to assess the association between continuous and categorical imaging parameters with a pathological diagnosis of RCC.

Two-sided *p*-values lower than 0.05 were considered statistically significant. All analyses were performed with SAS 9.4 (The SAS Institute, Cary, NC).

RESULTS

Patient characteristics

This study included 99 patients with 100 lesions. The median age of the patients studied was 66 years (range: 33 – 88 years), and 68.7 % (68/99) were males. No significant differences in age or gender were found between RCC and oncocytoma lesions (*p* > 0.95 for both) (Table 2). The mean time passed between the MDCT scan and the nephrectomy was 96 days (with minimum of 1 day and maximum of 331 days).

Lesion characteristics

Of the 100 renal lesions included in this study, 15 were oncocytomas (15%) and 85 were RCCs (85%). In the RCC group, 43

Figure 3. Multiphasic MDCT study (A) unenhanced phase, (B) corticomedullary phase, (C) nephrographic phase and (D): excretory phase of 44-year-old female shows a 3.7 cm solid lesion with homogeneous contrast enhancement in the middle third of the right kidney. ROIs were placed on the lesion and on the renal cortex in each phase, calculating the mean attenuation \pm SD. This lesion corresponded to an Oncocytoma. MDCT, multidetector CT; ROI, region of interest; SD, standard deviation.

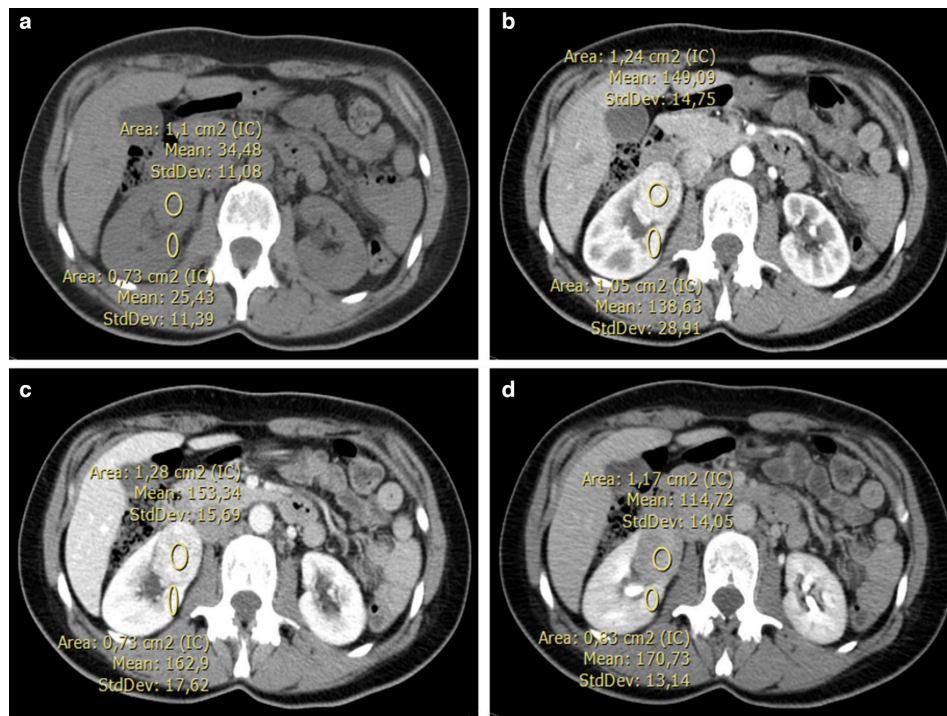


Table 2. Characteristics of patients and renal lesions

		All Patients	RCC	Oncocytoma	p-value
Lesions		100	85	15	
Patient characteristics					
Age (years)	Median (range)	65.5 (33 – 88)	66.0 (33 – 88)	68.0 (42 – 77)	> 0.95
Gender	Male	69 (69.0)	59 (69.4)	10 (66.7)	> 0.95
	Female	31 (31.0)	26 (30.6)	5 (33.3)	
Lesion characteristics					
Size (cm)	Median (range)	3.9 (1.2 – 19.0)	4.4 (1.3 – 19.0)	2.8 (1.2 – 9.1)	0.006
Calcifications	No	86 (86)	71 (83.5)	15 (100)	0.12
	Yes	14 (14)	14 (16.5)	0 (0)	
Cystic	No	84 (84)	71 (83.5)	13 (86.7)	> 0.95
	Yes	16 (16)	14 (16.5)	2 (13.3)	
Well defined	No	29 (29)	26 (30.6)	3 (20)	0.54
	Yes	71 (71)	59 (69.4)	12 (80)	
Enhancement	Heterogeneous	82 (82)	73 (85.9)	9 (60)	0.027
	Homogeneous	18 (18)	12 (14.1)	6 (40)	

RCC : renal cell carcinoma

Number represents frequency with percent of column in parentheses unless otherwise stated. Age and gender for all patients are out of 99 lesions, whereas all other measurements in the table are out of 100 lesions.

Table 3. Imaging of RCC and oncocytomas

	All Patients	RCC	Oncocytoma	p-value
Attenuation (HU)				
Unenhanced (N0)	30 (9 – 47)	30 (9 – 47)	28 (12 – 38)	0.34
Corticomedullary (N1)	85 (12 – 234)	85 (12 – 234)	87 (31 – 189)	0.59
Nephrographic (N2)	83 (26 – 229)	82 (26 – 229)	95 (41 – 150)	0.30
Excretory (N3)	65 (20 – 157)	63 (20 – 140)	72 (41 – 157)	0.08
Difference in attenuation (N-N0)				
Corticomedullary (N1-N0)	52.5 (1.0 – 200.0)	53.0 (1.0 – 200.0)	51.0 (19.0 – 151.0)	0.40
Nephrographic (N2-N0)	56.0 (12.0 – 201.0)	53.0 (12.0 – 201.0)	63.0 (26.0 – 114.0)	0.16
Excretory (N3-N0)	34.5 (9.0 – 124.0)	31.0 (9.0 – 112.0)	42.0 (26.0 – 124.0)	0.015
Ratio of attenuation (N/C)				
Unenhanced(R0)	1.07 (0.35 – 3.30)	1.10 (0.35 – 3.30)	1.00 (0.50 – 1.57)	0.13
Corticomedullary(R1)	0.75 (0.12 – 2.10)	0.76 (0.12 – 2.10)	0.70 (0.35 – 1.67)	0.73
Nephrographic(R2)	0.62 (0.20 – 1.14)	0.62 (0.20 – 1.14)	0.62 (0.35 – 0.99)	0.35
Excretory(R3)	0.61 (0.19 – 1.26)	0.61 (0.19 – 1.26)	0.69 (0.43 – 0.87)	0.07
Difference in attenuation ratios (N/C - N0/C0)				
Corticomedullary(R1-R0)	- 0.31 (-1.49 – 0.85)	- 0.33 (-1.49 – 0.85)	- 0.17 (-0.94 – 0.82)	0.29
Nephrographic(R2-R0)	- 0.43 (-2.79 – 0.57)	- 0.48 (-2.79 – 0.57)	- 0.22 (-0.97 – 0.25)	0.035
Excretory(R3-R0)	- 0.44 (-2.76 – 0.41)	- 0.47 (-2.76 – 0.41)	- 0.30 (-1.05 – 0.33)	0.021

RCC, renal cell carcinoma.

Numbers represent median with range in parentheses.

were clear cell RCCs and 37 were low-grade RCCs, including papillary and chromophobe subtypes. In addition, there were three mixed RCC (one chromophobe +papillary, one clear cell + chromophobe + papillary and one clear cell +papillary), one multilocular cystic RCC and one mucinous tubular RCC.

Tumor size

Tumor size was significantly larger in RCC lesions (median: 4.4, range: 1.3 – 19.0) compared to oncocytomas (median: 2.8, range: 1.2 – 9.1, $p = 0.006$).

Pattern of enhancement

RCC lesions had a higher proportion of heterogeneous enhancement (85.9%, 73/85) compared to oncocytomas (60%, 9/15) ($p = 0.027$) (Table 2).

Magnitude of enhancement

Table 3 shows the continuous imaging parameter measurements overall and by pathologic type.

Difference between mean enhancement of the lesion and baseline attenuation (N-N0)

The difference in attenuation between the excretory and the unenhanced phase (N3-N0) was significantly lower in RCC lesions (median: 31.0, range: 9.0–112.0) compared to oncocytomas (median: 42.0, range: 26.0–124.0) ($p = 0.015$).

Figures 3 and 4 show examples of lesions in each group.

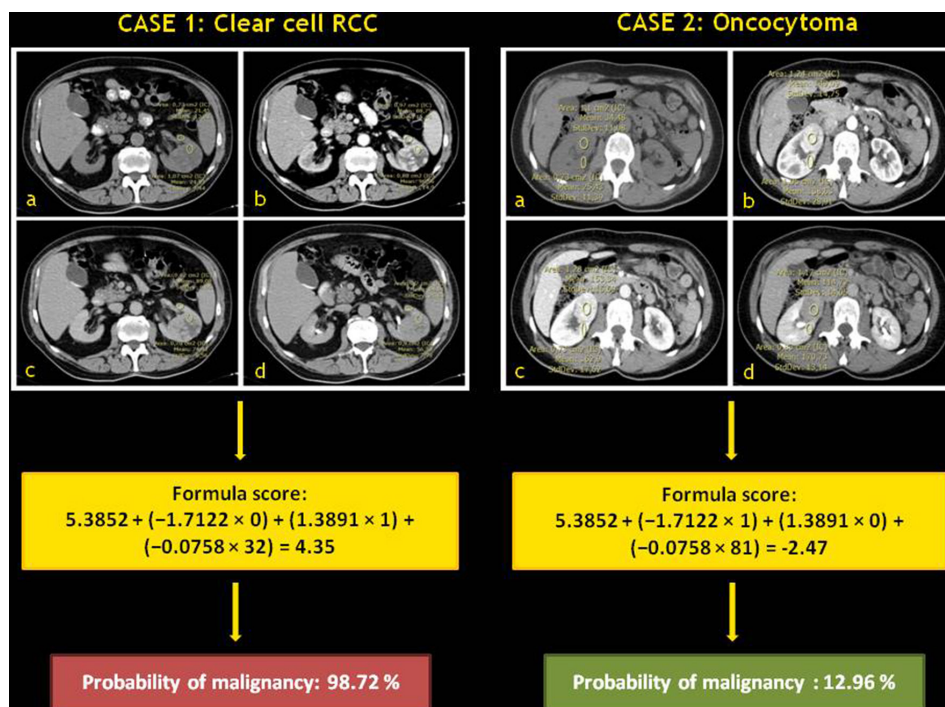
Multivariable predictive model validation in a new sample

The univariable and multivariable findings of the previous model are shown in Table 4. Similar to the previous findings published, the difference in the excretory phase compared to baseline remained significantly associated with the pathologic type, with a larger difference in the excretory phase compared to the unenhanced phase being associated with a lower probability of being RCC [oddsratio (OR): 0.96, 95% confidence interval (CI): 0.93 – 0.99, $p = 0.005$]. Similarly, homogeneous lesions had a significantly lower odds ratio of being RCC lesions (OR: 0.16, 95% CI: 0.03 – 0.75, $p = 0.020$) and lesions larger than 4 cm had a significantly higher probability of being RCC (OR: 5.89, 95% CI: 1.10 – 31.58, $p = 0.038$). The multivariable model developed in the previous study combining these parameters obtained an AUC of 0.85 (95% CI: 0.77 – 0.92), indicating very good discrimination performance of the model in this new sample (Figure 1).

DISCUSSION

The results of this study confirm that the previously developed multivariable model, that combines size, enhancement pattern, and difference in attenuation for the excretory phase, can correctly classify solid renal lesions such as RCCs and oncocytomas in 85% of the cases, confirming and validating results obtained in the previous work assessed.⁵ In addition, given the higher risk shown by the univariable analysis (OR: 7.31 [1.55 to 34.40] $p = 0.012$), a tumor size > 4 cm should always be taken into account as the first step in the absence of

Figure 4. Example of multivariate model application with the cases shown previously on Figure 1 and 2.



other imaging data and deserves to be further explored. We consider that this multiparametric approach using MDCT has a higher accuracy for differentiating these types of tumors than previous approaches reported in the literature^{4,6,7} in which these variables were analyzed independently. Despite the theoretical mathematical complexity of the formula, the application in the daily routine practice is simple. In order to facilitate its application we attach a spreadsheet, in which it has to be filled with the four parameters explained previously (its application can be performed in less than 1 min).

Different groups of patients could benefit from the application of this model, particularly those with lesions smaller than 4 cm, which is currently one of the most common scenarios in the clinical practice. Despite the fact that the American Urological Association has recently included the indication for biopsy of lesions in which the biopsy result can change the clinical management,^{8,9} this indication is not generally included in European urological guidelines.¹⁰ In these guidelines, biopsy is not considered necessary in patients undergoing surgery for enhancing solid lesions. However, biopsy is recommended when a benign lesion is suspected. In these cases, the predictive model could help support the decision to perform the biopsy if the result of the predictive model is a suspicion of oncocytoma. In addition, the predictive model can be useful in the management of patients in whom a biopsy is recommended but cannot be performed due to technical difficulties (in small lesions located in superior and anterior or internal leaflets)¹¹ or to comorbidities such as severe coagulation disorders. The suspicion of an oncocytoma can support a conservative management approach like active surveillance.

Despite the magnitude of enhancement remaining, the most studied independent variable for differentiation between RCCs and oncocytomas, there is still a lack of consensus about the optimal phase for this purpose. This is probably due to the heterogeneity that we observed in the MDCT protocol acquisitions (involving the number of phases, time of acquisition since the arrival of the contrast, etc.). Some studies such as that by Coy et al reported significant differences in arterial phase enhancement, considering this to be the optimal phase to help in this differentiation.^{12,13} However, our study suggests that the arterial phase is not helpful to differentiate RCC from oncocytoma, with the baseline and excretory phases being the most useful. Zhang et al.¹⁴ found no differences in excretory phase enhancement and also observed that both RCCs and oncocytomas are hypervascular in the nephrographic phase (the arterial phase was not evaluated), concluding that no differentiation could be made between RCCs and oncocytomas. Similar to the previous study, in this new sample the excretory phase remained the optimal phase to distinguish these tumors, being especially relevant the difference of attenuation (N3-N0; $p = 0.015$) and the difference in attenuation ratios (R3-R0; $p = 0.021$) of the nodule in the excretory phase compared to the baseline phase. This fact, and especially the difference in attenuation ratios, allow the results to be standardized independently of the equipment used or the amount of contrast administered, and also independently of the characteristics of the patients (such as cardiac function), similar to what has been reported in other studies.^{6,7} This relevant difference in contrast enhancement behavior between RCCs and oncocytomas could be explained by the latter characteristically showing a lower degree of washout in late phases. Lee-felker et al⁶ compared the degree of washout between the different phases in RCCs and oncocytomas and reported that the optimal parameter

Table 4. Risk of malignancy estimated by univariable and multivariable logistic regression models considering significant variables from the standard univariable analysis and AUC-ROC

		Univariable				Multivariable			
		OR	[95% CI]		p-value	OR	[95% CI]		p-value
Size > 4 cm	> 4 cm	7.31	[1.55 -	34.40]	0.012	5.89	[1.10 -	31.58]	0.038
	<= 4 cm	REF				REF			
Enhancement	Homogeneous	0.25	[0.07 -	0.82]	0.022	0.16	[0.03 -	0.75]	0.020
	Heterogeneous	REF				REF			
Size		1.47	[1.04 -	2.07]	0.028	---			
Unenhanced (N0)		1.04	[0.97 -	1.11]	0.25	---			
Corticomedullary (N1)		1.00	[0.99 -	1.01]	0.55	---			
Nephrographic (N2)		0.99	[0.98 -	1.01]	0.43	---			
Excretory (N3)		0.98	[0.96 -	1.00]	0.06	---			
Corticomedullary (N1-N0)		1.00	[0.98 -	1.01]	0.42	---			
Nephrographic (N2-N0)		0.99	[0.98 -	1.01]	0.29	---			
Excretory (N3-N0)		0.97	[0.95 -	1.00]	0.021	0.96	[0.93 -	0.99]	0.005
Unenhanced (R0)		4.52	[0.64 -	32.07]	0.13	---			
Corticomedullary (R1)		1.26	[0.25 -	6.24]	0.78	---			
Nephrographic (R2)		0.24	[0.01 -	4.89]	0.35	---			
Excretory (R3)		0.06	[0.00 -	2.90]	0.15	---			
Corticomedullary (R1-R0)		0.46	[0.11 -	1.88]	0.28	---			
Nephrographic (R2-R0)		0.19	[0.03 -	1.13]	0.07	---			
Excretory (R3-R0)		0.17	[0.03 -	1.01]	0.052	---			

AUC, area under the curve; 95% CI, 95% confidence interval; OR, odds ratio; ROC, receiver operating characteristic.

for their differentiation was the absolute de-enhancement value from the corticomedullary to the nephrographic phase. Perhaps the differences with our work might be explained by the acquisition time of the excretory phase, taking into account that in the Lee-Felker et al study the excretory phase was acquired at 8 min after contrast injection, whereas in our study it was acquired at 3 min. Other studies have also evaluated the degree of washout between different phases but did not include the excretory phase.¹⁵

Another possible source of discordance among the different studies depends on manual placement of the region of interest (ROI). Subjectivity of ROI placement can generate inherent variations, both in the detection of

the area of greatest uptake as well as in the size of the ROI. This problem could be solved by performing a voxel that includes the entire lesion.¹⁶ However, the use of this voxel manually requires additional analysis time. New software is being developed that segments the tumor automatically, simplifying the optimal placement of the ROI by automated algorithms (CAD), such as that described by Coy et al.¹² However, we obtained a higher AUC value compared to this method in the differentiation of RCC vs oncocytoma (0.85 vs 0.79, respectively). In addition, other new resources of CT image analysis currently under investigation, such as texture analysis, could be the key to the development of a new multiparametric predictive model.¹⁷

Similar to the results of the previous study, in the present study other parameters besides the enhancement pattern were significant and have already been described in the literature as being more suggestive of RCC than oncocytoma. In our cohort, the most significant parameter for tumor discrimination was again the size, with the mean (SD) size of RCCs being larger than oncocytomas (4.4 cm vs 2.8 cm, respectively; p 0.006).

This finding agrees with reports by authors such as Thompson et al, who stated that the risk of malignancy and tumor grade are correlated to tumor size.^{18,19} Nevertheless, when tumor size is evaluated separately, this parameter alone cannot help distinguish malignant from benign tumors and is not a reliable predictor of malignancy.²⁰ In fact, cases of small-sized tumors (<4 cm) with metastasis have been described in the literature.²¹

However, we consider that the association of size with other qualitative parameters, such as the enhancement pattern (homogeneous vs heterogeneous), is useful for the development of a predictive model. A heterogeneous enhancement pattern has been associated with malignant renal lesions, particularly in the case of the RCC subtype.²² In our study, RCCs were also more heterogeneous lesions than oncocytomas (85.9% vs 60%, respectively; p = 0.027). However, the tumor enhancement pattern is generally associated with its size, which is related to necrosis or hemorrhage being more commonly found in larger tumors.

The limitations of this study include its retrospective nature and the small number of oncocytomas included.¹⁹ However, our small sample should be viewed in the context of the low prevalence of these lesions. Other studies have reported similar or even smaller series of patients.^{4,13,14,23} Further, the lower bound of our AUC confidence interval (0.77) is still indicative of the good discrimination capacity of the model. We welcome the opportunity for future studies that involve additional treatment centers or have a wider time interval to increase the number of oncocytomas and allow for further validation of the predictive model. A theoretical limitation of this study is the utilization of different scanners. However, the positive result that we have obtained with this model could support its validation in the clinical daily practice. Another limitation is that analysis of different RCC subtypes was not made. We have not made the differentiation between the different histological subtypes of RCC because the objective of this work is allowing to suggest if a renal lesion is benign or malignant, regardless of the RCC subtype.

In conclusion, this study validates the usefulness of a MDCT predictive model (including parameters such as size, homogeneity and enhancement differences between the excretory and the baseline phases) in the differentiation between RCCs and oncocytomas.

REFERENCES

1. Society AC Cancer facts & figures 2018. *Cancer Facts Fig*2018; **2018**.
2. Nicolau C, Aldecoa I, Bunesch L, Mallofre C, Sebastia C, Saunders HS, et al. The role of contrast agents in the diagnosis of renal diseases. *Curr Probl Diagn Radiol*1995; **44**: 346–59.
3. Choudhary S, Rajesh A, Mayer NJ, Mulcahy KA, Haroon A. Renal oncocytoma: CT features cannot reliably distinguish oncocytoma from other renal neoplasms. *Clin Radiol*2009; **64**: 517–22. doi: <https://doi.org/10.1016/j.crad.2008.12.011>
4. Davidson AJ, Hayes WS, Hartman DS, McCarthy WF, Davis CJ. Renal oncocytoma and carcinoma: failure of differentiation with CT. *Radiology*1993; **186**: 693–6. doi: <https://doi.org/10.1148/radiology.186.3.8430176>
5. Paño B, Macías N, Salvador R, Torres F, Buñesch L, Sebastia C, et al. Usefulness of MDCT to differentiate between renal cell carcinoma and oncocytoma: development of a predictive model. *AJR Am J Roentgenol*2016; **206**: 764–74. doi: <https://doi.org/10.2214/AJR.15.14815>
6. Lee-Felker SA, Felker ER, Tan N, Margolis DJA, Young JR, Sayre J, et al. Qualitative and quantitative MDCT features for differentiating clear cell renal cell carcinoma from other solid renal cortical masses. *AJR Am J Roentgenol*2014; **203**: W516–24. doi: <https://doi.org/10.2214/AJR.14.12460>
7. Young JR, Margolis D, Sauk S, Pantuck AJ, Sayre J, Raman SS. Clear cell renal cell carcinoma: discrimination from other renal cell carcinoma subtypes and oncocytoma at multiphasic multidetector CT. *Radiology*2013; **267**: 444–53. doi: <https://doi.org/10.1148/radiol.13112617>
8. Campbell S, Uzzo RG, Allaf ME, Bass EB, Cadeddu JA, Chang A, et al. Renal mass and localized renal cancer: AUA guideline. *J Urol*2017; **198**: 520–529. doi: <https://doi.org/10.1016/j.juro.2017.04.100>
9. Lim CS, Schieda N, Silverman SG. Update on indications for percutaneous renal mass biopsy in the era of advanced CT and MRI. *AJR Am J Roentgenol*2019; **212**: 1187–96. doi: <https://doi.org/10.2214/AJR.19.21093>
10. Ljungberg B, Albiges L, Abu-Ghanem Y, Bensalah K, Dabestani S, Fernández-Pello S, et al. European association of urology guidelines on renal cell carcinoma: the 2019 update. *Eur Urol*2019; **75**: 799–810. doi: <https://doi.org/10.1016/j.eururo.2019.02.011>
11. Seager MJ, Patel U, Anderson CJ, Gonsalves M. Image- Guided biopsy of small (\leq 4 cm) renal masses: the effect of size and anatomical location on biopsy success rate and complications. *Br J Radiol*2018; **91**: 20170666. doi: <https://doi.org/10.1259/bjr.20170666>
12. Coy H, Young JR, Douek ML, Brown MS, Sayre J, Raman SS. Quantitative computer-aided diagnostic algorithm for automated detection of peak lesion attenuation in differentiating clear cell from papillary and chromophobe renal cell carcinoma, oncocytoma, and fat-poor angiomyolipoma on multiphasic multidetector CoM. *Abdom Radiol*2017; **42**: 1919–28.
13. Bird VG, Kanagarajah P, Morillo G, Caruso DJ, Ayyathurai R, Leveillee R, et al. Differentiation of oncocytoma and renal cell carcinoma in small renal masses (<4 cm): the role of 4-phase computerized tomography. *World J Urol*2011; **29**: 787–92. doi: <https://doi.org/10.1007/s00345-010-0586-7>
14. Zhang J, Lefkowitz RA, Ishill NM, Wang L, Moskowitz CS, Russo P, et al. Solid renal

- cortical tumors: differentiation with CT. *Radiology*2007; **244**: 494–504. doi: <https://doi.org/10.1148/radiol.2442060927>
15. Sasaguri K, Takahashi N, Gomez-Cardona D, Leng S, Schmit GD, Carter RE, et al. Small (< 4 cm) Renal Mass: Differentiation of Oncocytoma From Renal Cell Carcinoma on Biphasic Contrast-Enhanced. *AJR*2015; **205**: 205.
16. Chen F, Gulati M, Hwang D, Cen S, Yap F, Ugwueze C, et al. Voxel- Based whole-lesion enhancement parameters: a study of its clinical value in differentiating clear cell renal cell carcinoma from renal oncocytoma. *Abdom Radiol*2017; **42**: 552–60. doi: <https://doi.org/10.1007/s00261-016-0891-8>
17. Zhang G-M-Y, Shi B, Xue H-D, Ganeshan B, Sun H, Jin Z-Y. Can quantitative CT texture analysis be used to differentiate subtypes of renal cell carcinoma? *Clin Radiol*2019; **74**: 287–94. doi: <https://doi.org/10.1016/j.crad.2018.11.009>
18. Thompson RH, Kurta JM, Kaag M, Tickoo SK, Kundu S, Katz D, et al. Tumor size is associated with malignant potential in renal cell carcinoma cases. *J Urol*2009; **181**: 2033–6. doi: <https://doi.org/10.1016/j.juro.2009.01.027>
19. Frank I, Blute ML, Cheville JC, Lohse CM, Weaver AL, Zincke H. Solid renal tumors: an analysis of pathological features related to tumor size. *J Urol*2003; **170**(6 Pt 1): 2217–20. doi: <https://doi.org/10.1097/01.ju.0000095475.12515.5e>
20. Mues AC, Landman J. Small renal masses: current concepts regarding the natural history and reflections on the American urological association guidelines. *Curr Opin Urol*2010; **20**: 105–10. doi: <https://doi.org/10.1097/MOU.0b013e32833625f8>
21. Lee H, Keun Lee J, Kim K, Kwak C, Hoe Kim H, Byun S-S, et al. Risk of metastasis for T1a renal cell carcinoma. 2016; **34**: 553–9.
22. Kim JK, Kim TK, Ahn HJ, Kim CS, Kim K-R, Cho K-S. Differentiation of subtypes of renal cell carcinoma on helical CT scans. *AJR Am J Roentgenol.* . 2002; **178**: 1499–506 2002/05/30. doi: <https://doi.org/10.2214/ajr.178.6.1781499>
23. Kim JI, Cho JY, Moon KC, Lee HJ, Kim SH. Segmental enhancement inversion at biphasic multidetector CT: characteristic finding of small renal oncocytoma. *Radiology*2009; **252**: 441–8. doi: <https://doi.org/10.1148/radiol.2522081180>